Research Article

Ming-Lang Tseng, Annson Thampy, Emad A. A. Ismail, Fuad A. Awwad, and Nima E. Gorji*

Heat treatment and tensile test of 3D-printed parts manufactured at different build orientations

https://doi.org/10.1515/phys-2023-0163
received October 20, 2023; accepted December 02, 2023

Abstract: Additive manufacturing has been gaining popularity in many industries and has made significant growth over the last 5 years. Many industries use additive manufacturing three-dimensional (3D) printing to produce complex shape objects that is a challenge to be manufactured by casting or conventional methods. In this study, the impact of heat treatment and build orientation is examined for the mechanical characteristics of 3D-printed parts. The study used samples constructed of titanium alloy Ti-6Al-4V, which is frequently used in AM applications. The parts were printed at various build orientations such as 0°, 45°, and 90°. Following printing, the samples underwent four distinct heat-treatments at 0, 700, 800, and 900°C. The variation in mechanical properties (Young's modulus, strain-stress, and tensile strength) has been monitored to determine the best heat treatment and tilt orientation to obtain the best mechanical properties. These findings provide a systematic analysis and support the 3D printing of the parts used with a desired mechanical strength.

Keywords: additive manufacturing, Ti-6Al-4V, built orientations, heat treatment, mechanical properties

*** Corresponding author: Nima E. Gorji,** Department of Mechatronic Engineering, Technological University Dublin, Dublin 15, Ireland, e-mail: nima.gorji@tudublin.ie

Ming-Lang Tseng: Institute of Innovation and Circular Economy, Asia University, Taichung City, Taiwan; Department of Industrial Engineering, Khon Kaen University, Khon Kaen, Thailand; Department of Medical Research, China Medical University Hospital, China Medical University, Taichung, Taiwan

Annson Thampy: School of Manufacturing Technology, South-East Technological University, Waterford, Ireland

Emad A. A. Ismail, Fuad A. Awwad: Department of Quantitative analysis, College of Business Administration, King Saud University, P.O. Box 71115, Riyadh 11587, Saudi Arabia

1 Introduction

3D printing conditions can considerably impact the quality, accuracy, and reliability of printed parts [1–4]. Specific printing configurations can vary depending on the printer model, material, and desired impact [5,6]. Three-dimensional (3D) printing has become a game-changer in various industries like healthcare, aerospace, automotive, and manufacturing. It is known for its ability to produce complex shapes and custom parts with precision, making it a popular choice for modelling and finished products. However, the building orientation of the object on the build plate plays a crucial role in achieving the desired quality and precision of the printed object. Building orientation refers to the angle and direction of the object on the build plate, and it affects the strength, surface quality, and precision of the finished product [7]. To achieve this, a heat treatment procedure is often used as a post-processing step. This involves heating the object to a specific temperature, holding it at that temperature for a certain period of time, and then cooling it down. By doing this, we can change the object's microstructure, which can improve its strength, ductility, and toughness [8,9]. Eryildiz *et al.* in their research studies clearly shows the variations in the ultimate tensile strength (UTS) and percentage of maximum elongation. Seven samples at different temperatures are used for the experimentation [10]. At the no heating or the built-in conditions, the UTS and yield strength (YS) are given as 1,191 and 908 MPa, respectively. As the temperature rises from 450 to 550°C the UTS increases the values to 1,198, 1,211, and 1,220 MPa, respectively. Similarly, the YS increases to 863, 890, and 917 MPa, respectively. Then, as the temperature rises to 600 and 650°C it shows a significant dip in the UTS and YS values as 1,167, 1,117, 886, and 879 MPa, respectively. On the other hand, the rate of elongation continuously increases as the temperature increases from 9.2 to 12.3%. It is evident that the optimum temperature at which it shows the maximum stress–strain values is at 550°C. After this temperature, the sample shows a significant dip in the values of both stress and strain. So, up to a certain temperature, the positive hike is clear and after that the stress and strain will decrease in the Ti-6Al-4V [11]. Zhilyaev *et al.* correlated the relationship between stress and strain relation at various post-heat treatment temperatures [12]. The effect of cooling the heated sample at various temperatures and by various cooling methods is clearly stated and studied in the previous research [13]. The ideal post-heat treatment candidate was found to be the solid solution, which was heated at 800°C for 2 h followed by water cooling plus aging at 500°C for 4 h followed by furnace cooling because it increased YS and UTS by 3.33 and 12.85%, respectively, while the tensile fracture elongation (EL) decreased by 3.37% in comparison to the samples that were not heated [14]. The maximum strain attained was at the time of post-heat treatment at 800°C for a period of 2 h with air cooling. But when the time of heat treatment was extended to 4 h, the strain tends to suddenly decrease but shows a hike in strength. This has opted as the optimum post-heat treatment temperature for the Ti-6Al-4V alloy to provide the maximum strength among all the heat treatment conditions. In contrast, in case of furnace cooling for the titanium alloy, the heating for 800°C for 2 h and 500°C for 4 h do not show any significant variation in the strain and is considered too minimal. However, heating for a long time at a less temperature tends to show an increase in the strength of the titanium alloy, rather than providing a high temperature for a short period of time. After a certain limit of increase in strength when the heating continues, it shows a sudden dip in the strength of the alloy. Gorji *et al.* in their research reported the particle size distribution of 316L powders used in 3D printing using tomography and microscopy, and nanoindentation [15].

In this study, 3D printed parts were manufactured at different tilt angles and were heat-treated at different temperatures. The parts were subject to ultimate tensile testing, strain-stress analysis, Young's modulus measurements, and surface roughness analysis both before and after heat treatment at various temperature levels. These comprehensive results provide a methodical assessment that supports the use of 3D printing to achieve desired mechanical strength in the fabricated components.

2 Experimental methodology

Based on the required parameters and print conditions as stated in Table 1, an EOS printer was used, and the 3D-printed parts are produced using Ti-6Al-4V alloy. The laser power was set at 160 W. The thickness of each layer is set to be 60 μm. The point distance that is the distance from the printing bed and the laser source is set to be 40 μm, this distance should be properly maintained to get the desired characteristics for the product. The laser exposure time is set to be 180 μs as increasing or decreasing the time may affect the quality of the printed part. The hatch spacing or the distance between each layer is set to be 90 μm. To obtain the desired shape as per the pre-designed programme, the scan speed is set to be 220 mm/s. The oxygen concentration is a vital component that needs to be properly maintained throughout the 3D printing process, and in this case, the oxygen concentration is set to be 0.1%. The laser spot size determines the amount of area in which the energy needs to be dissipated and, in this case, it is set as 75 μm. All these print conditions need to be properly maintained throughout the 3D printing process so that the decided characteristic of the product printed with titanium powder can be attained. All the physical and mechanical properties are thus studied based on the above pre-set conditions and temperature ranges. The parts were standard tensile test bars as shown in Figure 1.

Table 1: 3D Printing parameters used to print the parts

Print conditions	Parameters
Laser power (W)	160
Layer thickness (μm)	60
Point distance (μm)	40
Exposure time (μs)	180
Hatch spacing (μm)	90
Scan speed (mm/s)	220
Oxygen concentration (%)	0.1
Laser spot size (μm)	75

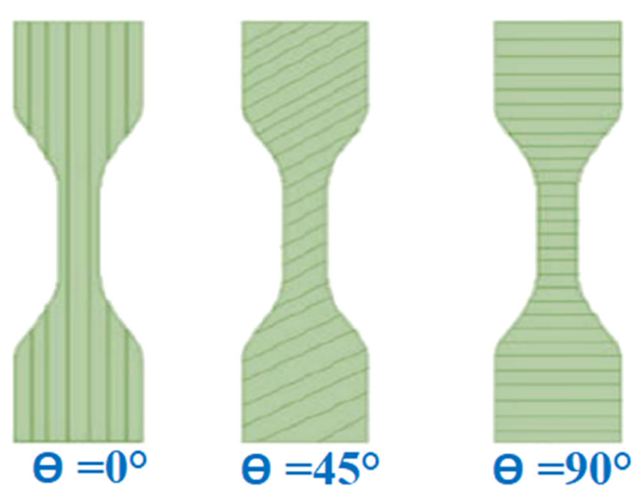

Figure 1: The tensile test bars printed at different build orientations.

3 Results and discussion

The following results are obtained after the experimentation using the alloy printed parts at various temperatures and build orientations.

3.1 Build orientation (*θ*)

The overall quality, mechanical characteristics, and functionality of printed products are significantly influenced by the construction orientation of the individual elements. The orientation in which a 3D printed part is placed or layered during the additive manufacturing process is called the build orientation. It entails how the part is positioned in relation to the build plate or printing platform. The SEM images taken from the parts printed at different build orientation has been shown in Figure 2. These images were processed by ImageJ [16–18]. Certain conclusions about the microstructural properties can be obtained by processing the SEM images.

Figure 3 shows the directionality histograms of the tensile bars printed at three different tilt orientations. The part printed at 90° orientation has shown less variation for a wider range of directions and therefore, is the best orientation to print the samples. The horizontally placed sample at 0**°** shows most variation at 0 direction and thus would negatively influence the mechanical properties of the sample.

3.2 Relationship between built orientation and surface roughness

Unevenness and deviations in a surface's texture can be referred to as surface roughness. Surface roughness is a key factor in influencing the quality and usefulness of the printed object when utilizing titanium powder for 3D printing of the parts especially for biomedical applications and aviation industry. Figure 4 shows the variation in surface roughness (obtained by AFM) at various build orientation angles for the 3D-printed parts.

It is understood that the surface roughness will be maximum at 0° printing angle which is 29 µm. At 45° printing angle, the surface roughness will be 6.5 µm and it will be the least roughness (0.4 µm) for parts printed vertically at 90° angle. At 0° and 45° tilt angles, the deposition of the melted particle will be uneven, and this may cause an increase in the surface roughness. So, in order to achieve a printed part with minimum surface roughness,

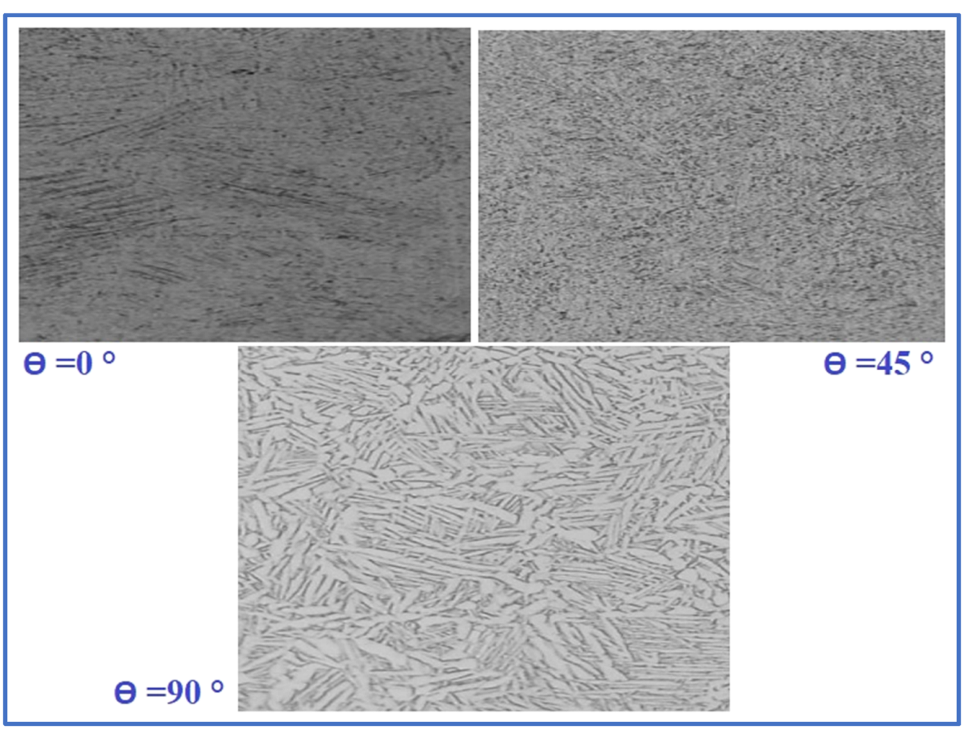

Figure 2: SEM image of the sample printed at *θ* = 0°, 45°, and 90° build orientations.

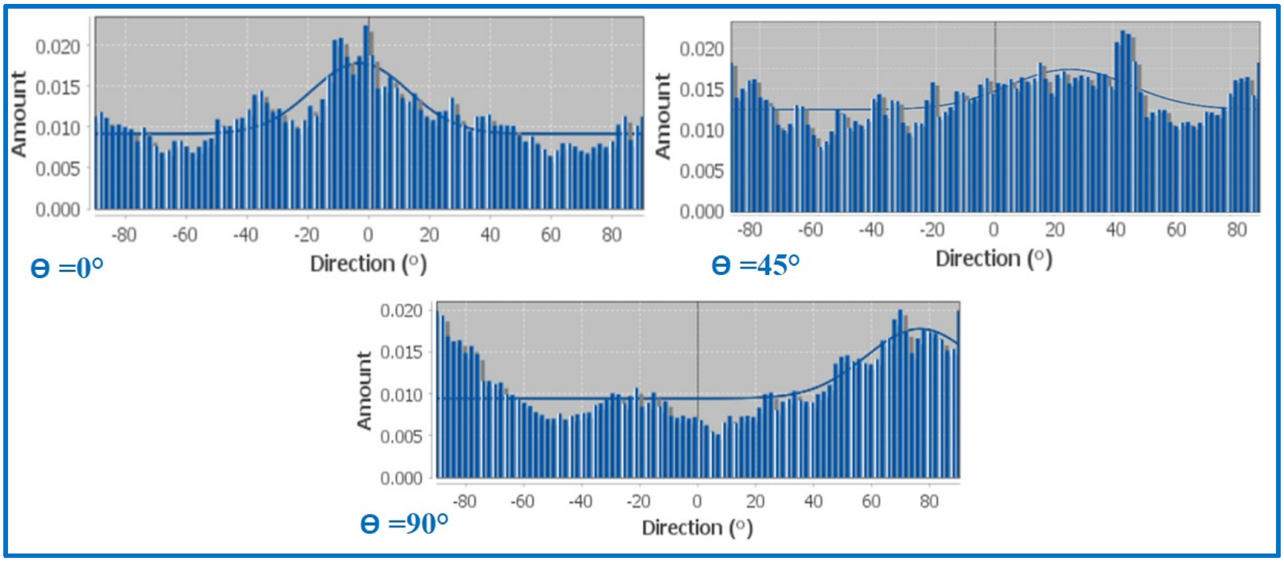

Figure 3: Directionality histogram for the tensile bars printed at 0°, 45°, and 90° tilt orientations.

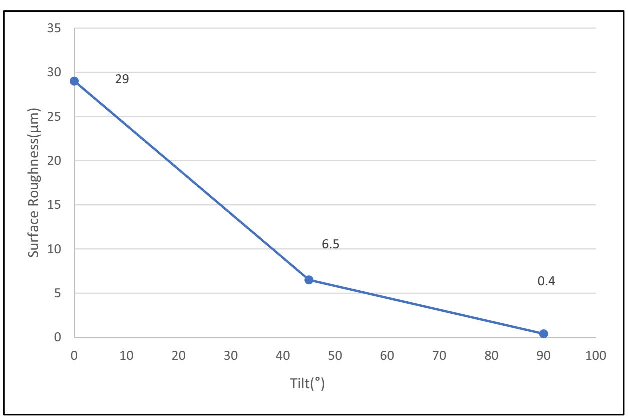

Figure 4: Variation in surface roughness *vs* the build tilt angle.

the build orientation should be selected as 90° to reduce the uneven melting of the particles and improved solidification post-print. At 0° and 45° tilt angles, the surface roughness tends to be higher compared to other angles due to the printing process's inherent characteristics and the orientation of the layers when utilizing titanium powder for 3D printing. At 0° and 45° angles, the layering of the material might result in a greater tendency for stair-stepping effects or unevenness between layers. This can cause an increased surface roughness due to the way the material is deposited and solidified in these orientations. Depending on the specific 3D printing technique used, supports might be needed to maintain stability during printing. At certain angles, such as 0° and 45°, the requirement for additional supports or the way they are applied might contribute to increased surface roughness. The angle of deposition at 0° and 45° could lead to a higher likelihood of material accumulation or uneven distribution, resulting in a rougher surface finish compared to other angles. The tool path followed by the 3D printer's nozzle or laser might be less optimized or less efficient at these angles, affecting the uniformity of material application and consequently causing higher surface roughness. The variations in surface roughness based on different build orientation angles in the 3D printing process are crucial to understand for industries like biomedical applications and aviation where surface quality directly impacts the functionality and reliability of the printed parts.

3.3 Build orientation, Young's modulus, and UTS

The build orientation in 3D printing defines the direction in which the material is arranged in layers all through the printing process. For titanium alloy, the connection between Young's modulus and UTS might change depending on its building orientation during 3D printing [19,20]. The elastic modulus, commonly referred to as Young's modulus (E_r), is a measurement of a material's stiffness or rigidity. It reflects the ability of a substance to endure temporary deformation caused by an applied load [21]. The maximum stress a material can withstand before breaking under tension is known as UTS. The values obtained during the experimentation are provided below.

Figure 5 shows the variation in Young's modulus in relation to build orientation at 0°, 45°, and 90°. The printing

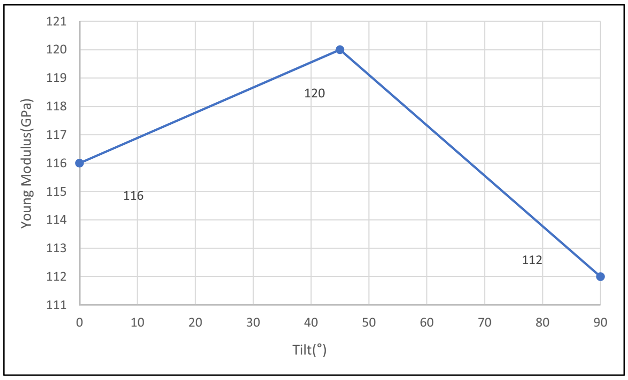

Figure 5: Variation in Young's modulus of the parts printed at different tilt orientations.

angle of 0° resulted in a E_r of 116 GPa. This suggests that the object printed at a flat orientation is stiffer material since E_r evaluates a material's stiffness or rigidity [21]. The value indicated on the graph at a 45° printing angle is 120 GPa. This implies that the object's stiffness rises to 120 GPa when it is constructed with a 45° orientation. This angle introduces some diagonal arrangement in the printed layers, perhaps affecting the material's mechanical properties. Finally, the noted value on the graph is 112 GPa at a printing angle of 90°. This shows that the object's rigidity drops to 112 GPa when it is constructed vertically. Comparing the vertical layer arrangement to flat or diagonal orientations may reveal a distinct mechanical behaviour. According to the information provided in the graph, it can be seen that the build orientation affects how rigid the printed object is. The 45° orientation results in the most rigidity, whereas the vertical (90°) orientation results in the lowest stiffness. According to these results, the object's printing angle significantly affects its mechanical characteristics, particularly its Young's modulus. The increase in stiffness to 120 GPa when the object is constructed with a 45° orientation compared to the 0° orientation (which had a stiffness of 116 GPa) could be attributed to the following factors: At a 45° printing angle, the layers are arranged diagonally. This diagonal arrangement introduces a different distribution of stresses across the printed layers compared to the flat (0°) orientation. The diagonal arrangement might create a more interlocked or supportive structure, potentially enhancing the material's stiffness. The diagonal layering at 45° could distribute applied loads more evenly throughout the structure compared to the flat orientation, resulting in an increased resistance to deformation and higher stiffness. The orientation at 45° might promote better interlayer bonding or increased contact area between adjacent layers, thereby improving the material's overall stiffness. The diagonal orientation might facilitate specific grain development or structural alignments within the printed material that contribute to increased stiffness compared to the 0° orientation. The 45° orientation might align stress lines more favourably, minimizing the propagation of stress through the material, thus enhancing its stiffness. These factors collectively suggest that the diagonal orientation at 45° introduces certain structural elements or load-bearing configurations that result in a higher Young's modulus (stiffness) of 120 GPa compared to the flat (0°) orientation. The changes in layer arrangement and stress distribution likely play a significant role in influencing the mechanical behaviour of the printed object, resulting in varying stiffness based on different build orientations.

Figure 6 shows the variation in UTS *vs* the build orientation of the titanium printed parts. Parts printed at three build orientations of 0°, 45°, and 90° have been tested. The utmost stress a material can endure before breaking under strain is referred to as UTS. In this instance, the stronger the material, the higher the UTS [22]. The material has an UTS of 1,150 MPa at a 0° build orientation. This shows that the material has great strength under tension when constructed with the layers aligned in a 0° direction. The UTS drops significantly to 1,120 MPa at 45° build orientation. This implies that the material's strength under strain is slightly decreased when the layers are aligned at a 45° tilt as opposed to a 0° horizontal orientation. The maximal tensile strength rises to 1,200 MPa at a 90° tilt orientation. This suggests that the material obtains some additional strength under stress compared to 0° and 45° orientation when the layers are oriented perpendicular to the loading direction (90°).

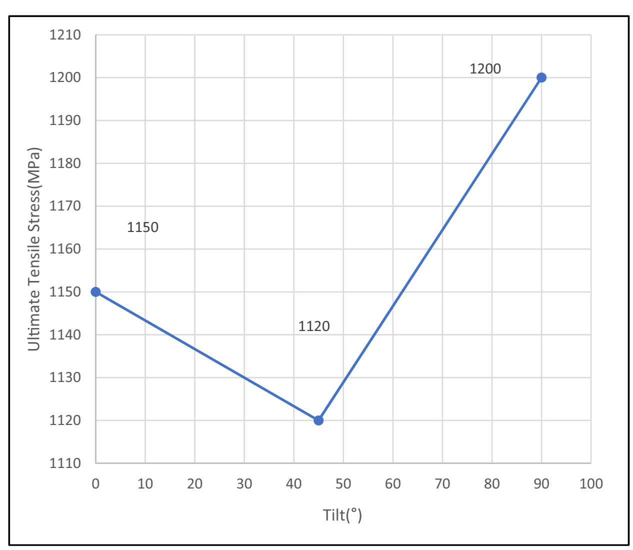

Figure 6: Variation in UTS by tilt of the part.

3.4 E_r and UTS at various heat treatment temperatures

In the context of titanium 3D printing, multiple factors, including the heat treatment temperature, may influence the relationship between E_r and UTS. In this section, all the parts printed at different build orientations (tilt) and tested for different heat treatment temperatures are described. The relation between heating temperature and Young's modulus is shown in Figure 7. A measurement of a material's stiffness or rigidity is said to be Young's modulus. It determines how much strain (deformation) a material experiences in response to a specific quantity of stress (force).

Specific points of interest are shown by the marked values on the graph. Young's modulus at 700°C is 112 GPa and rises to 120 GPa at 800°C and finally, decreases again to 110 GPa at 900°C. We can infer from this knowledge that Young's modulus, a measure of a material's stiffness, changes as the heating temperature rises. The material has a rigidity of 112 GPa at 700°C. The rigidity rises to 120 GPa as the temperature reaches 800°C. However, the rigidity marginally falls to 110 GPa at 900°C. The relationship between heating temperature and Young's modulus is that raising the heating temperature generally improves the material's stiffness. The fact that stiffness decreased as the temperature rises from 800 to 900°C suggests that overheating the parts may have an adverse impact on stiffness.

Figure 8 shows the correlation between the final tensile strength of the printed parts and the heating temperature. The UTS slightly decreases from 1,050 to 1,045 MPa as the heating temperature rises from 700 to 800°C. The UTS, however, dramatically increases to 1,070 MPa when the heating temperature is raised to 900°C. The substance has an UTS of 1,050 MPa at 700°C. This number represents the highest stress that a material can withstand before breaking or deforming in the presence of a tensile force. The material is suitable for applications needing strong structural integrity since a higher tensile strength indicates that it is more resistant to pulling forces. The UTS slightly reduces to 1,045 MPa at 800°C heating temperature. This modest loss in strength indicates that the material degrades or changes to some extent when the temperature rises. The material's UTS increases noticeably, reaching 1,070 MPa at the greatest heating temperature of 900°C. This increase in strength suggests that at certain temperatures, the material goes through a transition or strengthening mechanism. It could be explained by elements like enhanced atomic bonding, grain development, or a phase shift that improves the material's overall mechanical properties. Therefore, the heating temperature significantly affects the material's UTS. As the temperature increases from 700 to 800°C, the strength shows a minor decrease followed by a significant increase at 900°C [23]. The modest loss in UTS to 1,045 MPa at 800°C heating temperature indicates that the material undergoes some level of degradation or alteration when subjected to higher temperatures. This decrease in strength suggests that, at 800°C, certain changes or reactions occur within the material that affect its structural properties. The factors contributing to this slight reduction in UTS could include the following: Higher temperature might cause thermal degradation or chemical changes in the material, leading to a weakening of the atomic or molecular structure, which subsequently results in a reduction in tensile strength. Elevated temperatures can induce changes in the microstructure of

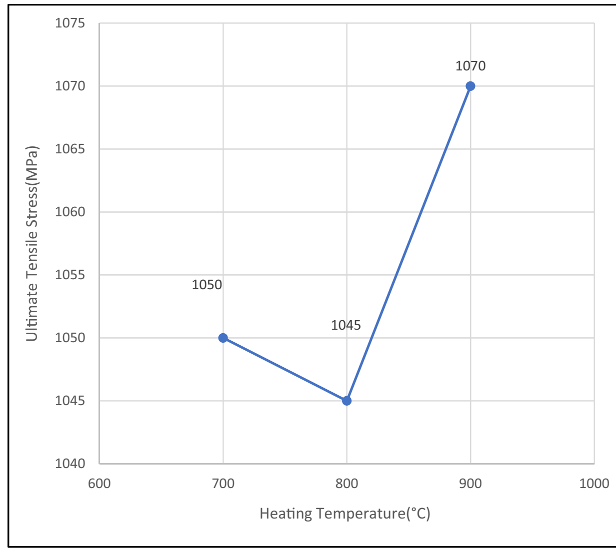

Figure 8: Variation in UTS due to post-printing heating temperature.

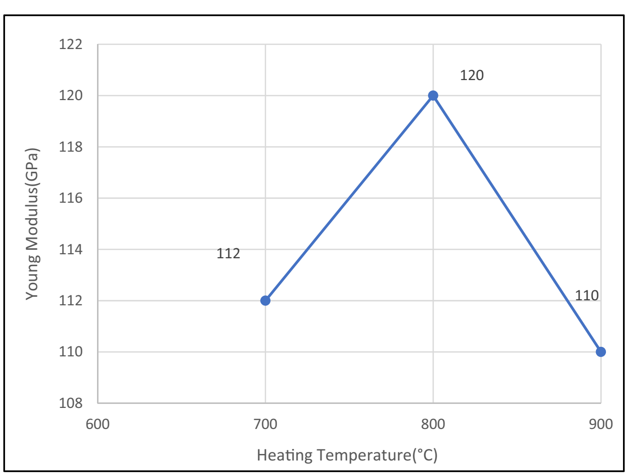

Figure 7: Variation in Young's Modulus of the printed parts after post-printing heating at different temperatures.

the material, such as grain growth, defects, or alterations in atomic arrangement, which can impact its mechanical properties, including tensile strength. The material might undergo a phase transformation or transition at 800°C, altering its crystal structure or arrangement, thereby affecting its mechanical behaviour and resulting in a slight decrease in UTS. The increased thermal energy at 800°C might cause a decrease in atomic bonding strength, resulting in a minor reduction in the material's tensile strength. The decrease in UTS from 1,050 MPa at 700°C to 1,045 MPa at 800°C indicates that the material experiences some changes or degradation at this temperature, although the effect is relatively modest compared to the subsequent substantial increase observed at 900°C.

3.5 Stress–strain and heat treatment temperature

Stress is a measurement of the internal forces that external loads or forces have on a material. It displays the magnitude of the force per unit area acting on the cross-sectional area of the material. Depending on the type of applied pressure, stress can be divided into several types, such as tensile stress, compressive stress, shear stress, and more [24,25]. On the other hand, strain is a measurement of the lengthening or distortion that takes place in a material as a response of stress. It measures the proportionate change in the material's size or form because of external forces. Strain is a dimensionless quantity that can be stated as a ratio or percentage. It shows how much the material's length or size has changed in relation to the direction of the applied force.

Figure 9 shows the relationship between the stress and strain at various heating temperatures. It is clearly seen

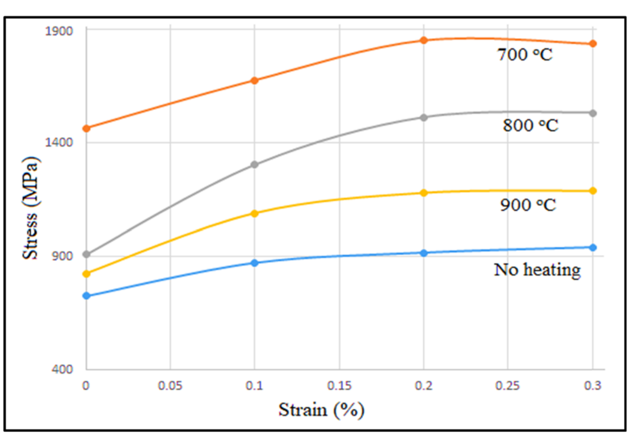

Figure 9: The relation between stress and strain at various post-printing heating temperatures.

that at various temperatures, the sample is reacting differently within each range of temperature. As per the values obtained during the experimentation, the sample at no heating condition shows minimal stress–strain variations as compared to the other temperature ranges. It is significant to highlight that the stress and strain relationship does not consider variables like temperature effects, thermal expansion, or time-dependent behaviour, which may be relevant under different circumstances when there is no heating. When a sample is subjected to no heating or ambient temperature conditions, it tends to exhibit minimal stress–strain variations due to several reasons, at ambient or room temperature, the material properties remain relatively stable and uniform throughout the sample. The absence of elevated temperatures means that the material's internal structure remains unchanged, leading to consistent behaviour in stress and strain responses. Without any heating, there are no thermal gradients or alterations in the material's microstructure, which often cause variations in mechanical properties. The absence of these thermal effects maintains the material's integrity and consistency in stress–strain behaviour. Heating typically leads to thermal expansion or contraction within the material, which can introduce stress points or induce changes in the sample's dimensions. In a no-heating scenario, the absence of thermal fluctuations prevents these variations, resulting in minimal stress–strain changes. When testing samples at room temperature or in a controlled environment without heating, the consistent and stable conditions contribute to minimal fluctuations in stress and strain, allowing for more predictable and uniform mechanical responses. Without external factors like high temperatures, the sample remains in a relatively static state, reducing the likelihood of dynamic changes in the material's properties, and hence, minimizing stress–strain variations. In summary, no heating conditions maintain the material in a stable state, preserving its structural integrity and uniformity, resulting in minimal stress–strain variations during testing. This stability provides a baseline understanding of the material's mechanical behaviour under standard or ambient temperature conditions.

Table 2 presents all the measurements repeated on the samples after heat-treatment at different temperatures. The trend is not different when the experiments are repeated. The mechanical reaction of a material to external forces within its elastic range is described by stress and strain at no heating circumstances. At 700°C, the stress–strain relation shows its maximum values at the experimentation stage. Starting from 565.02 MPa stress at 0 strain and slowly increases to 1853.57 MPa at 0.3% strain and decreases to 1683.1 MPa. On the other hand, at 800°C the stress–strain relation starts at a very low value of

Table 2: Experimental values of stress and strain at various heating temperatures

Strain (MPa)	Stress (%), no heating	Stress (%) at 700°C	Stress (%) at 800°C	Stress (%) at 900°C
0	47.83277	565.02	17.94	23.92
0	346.7864	1061.29	517.19	508.22
0	726.4575	1464.87	908.82	825.11
0.1	872.9448	1677.13	1303.44	1091.18
0.1	905.8297	1736.92	1431.99	1156.95
0.1	902.8402	1751.87	1452.91	1133.03
0.2	932.7355	1826.61	1467.86	1162.93
0.2	917.7878	1853.51	1512.71	1180.87
0.3	941.7041	1838.57	1533.63	1189.84
0.3	810.1645	1683.11	1509.72	1052.32
0.3	1145.79	1683.11	1210.76	914.8

17.94 MPa which then subsequently shows a rise to a maximum of 1509.72 MPa and gradually decreases to 1210.76 MPa. Moreover, at 900°C, the value of stress is 23.92 MPa at 0 strain and it also shows a gradual hike to 1189.84 MPa at a higher strain of 0.3% and then falls to a value of 914.80 MPa. Thus, for the parts printed using titanium powder, it can be concluded that at 900°C, there is a minimum variation in stress and strain. Thus, it will be subjected to more deformation at this temperature. But when not heated it shows the least deformation values. At 700°C, it shows that the particle can withstand more deformation when subjected to mechanical testing. As the temperature rises, the printed parts show less strength and are highly prone to mechanical deformation [26].

4 Conclusion

Several tensile test bars were 3D printed at various tilt orientations and were subjected to post-print heat treatment. The heat-treated parts were then characterized for surface roughness, mechanical strength, and SEM microstructure analysis. The UTS and Young's modulus, surface roughness results, and strain–stress analysis were performed for the parts printed at three tilt orientations (0°, 45°, and 90°). At 0° tilt, the UTS of the part was 1,150 MPa and shows the maximum surface roughness of 29 µm and a Young's modulus of 116 GPa. But at 45°, the Young's modulus reaches a maximum value of 120 GPa and the surface roughness reduces significantly to 6.5 µm. However, the 90° tilt resulted in a better mechanical strength as UTS raised to a high value of 1,200 MPa and very less surface roughness of 0.4 µm was obtained. The Young's modulus value is also at the lowest, 112 GPa. From these results, we can conclude that the 90° print angle (vertical printing) is the best printing angle at least for printing the parts from titanium alloy with the given printing parameters. Furthermore, the stress and strain are at maximum at 700°C and the UTS and Young's modulus values are 1,050 MPa and 112 GPa, respectively. Finally at 900°C, the UTS value is maximum, *i.e.*, 1,070 MPa. This material deformation at a high temperature led to a decrease in the stress–strain values which reduce the UTS of the material. So, from this, it is evident that titanium alloys are best suited to be heat treated for a particular range of temperature (800°C), but when further heated, the strength of the titanium print parts decreases. When comparing these temperatures, the maximum value of Young's modulus, which is 120 GPa, showing maximum elasticity, is obtained at 800°C . At 700°C the value is 112 GPa and shows a surge at 800°C and then when the temperature is increased further to 900°C, the Young's modulus decreases to 110 GPa. Based on the comparison with the various literature and the experimental findings, it is evident that the stress–strain or the strain-strength relations will be positive only up to a certain limit of temperature as in the case of the titanium alloy. This limit depends on the size, shape, and other physical properties of the 3D-printed object. The titanium alloy can only hold stress up to a certain limit after which the stress reduces drastically. In agreement with other literature, we reported that the desired mechanical properties of 3D printed parts can be attained by proper adjustment of printing orientation and post-print heat treatment temperature.

Acknowledgments: Researchers Supporting Project number (RSPD2024R1060), King Saud University, Riyadh, Saudi Arabia.

Funding information: Researchers Supporting Project number (RSPD2024R1060), King Saud University, Riyadh, Saudi Arabia.

Author contributions: All authors have accepted responsibility for the entire content of this manuscript and approved its submission.

Conflict of interest: The authors state no conflict of interest.

References

[1] Vock S, Klöden B, Kirchner A, Weißgärber T, Kieback B. Powders for powder bed fusion: A review. Prog Addit Manuf. 2019;4:383.

[2] Michaela F, Dalibor V. Thermal treatment of 3D-printed titanium alloy. Manuf Tech. 2018;18:277.
[3] Yi Z, William J, Yeon-Gil J, Jing Z. Additive manufacturing processes and equipment. Addit Manuf. 2018;1:39.
[4] Alexandra A, Robert F, Thomas E, Florian P. Powder metallurgy strategies to improve properties and processing of titanium alloys. Adv Energ Mat. 2017;19(6):1600743.
[5] Slotwinski JA, Garboczi EJ, Stutzman PE, Ferraris CF, Watson SS, Peltz MA. Characterization of metal powders used for additive manufacturing. J Res Natl Inst Stand Technol. 2014;119:460.
[6] Altatu M, Cristiana C. Effect of heat treatment on some titanium alloys used as biomaterials. Appl Sci. 2022;12(21):11241.
[7] Novana H, Miller WS, Ahmad Z. Effects of build orientation and heat treatment on microstructure, mechanical and corrosion properties of Al6061 aluminium parts built by cold spray additive manufacturing process. Intl J Mech Sci. 2021;204:106526.
[8] Hartunian P, Eshraghi M. Effect of build orientation on the microstructure and mechanical properties of selective laser-melted Ti-6Al-4V alloy. J Manuf Mater Proc. 2018;2(4):69.
[9] Lin JW, Feng KY, Tekdir H, Hu JY, Zhao Z, Huang L. The effect of a novel low-temperature vacuum heat treatment on the microstructure and properties of Ti–6Al–4V alloys manufactured by selective laser melting. Vacuum. 2021;193:110554.
[10] Eryildiz M. Effect of build orientation on mechanical behaviour and build time of FDM 3D-printed PLA Parts: An experimental investigation. Eur Mech Sci. 2021;5:116.
[11] Bermingham M, Xue A, Lin Z, Welsch G. Microstructure-gradient approach for effective determination of post-heat treatment temperature of an additive manufactured Ti-6Al-4V sample. J All Comp. 2022;921:165630.
[12] Zhilyaev AP, Ringot G, Huang Y, Cabrera JM, Langdon TG. Mechanical behaviour, and microstructure properties of titanium powder consolidated by high-pressure torsion. Mater Sci Eng A. 2017;688:498–504.
[13] Mueller J, Shea K. The effect of build orientation on the mechanical properties in inkjet 3D-printing. In: Proceedings of International Solid Freeform Fabrication (SFF) Symposium 26. Austin, USA; 2015. p. 983–90.
[14] Baltatu MS, Cristiana C. Effect of heat treatment on some titanium alloys used as biomaterials. J Mater Eng Perform. 2022;12:11241.
[15] Gorji NE, Robert R, Dermot B. X-ray tomography, AFM and nanoindentation measurements for recyclability analysis of 316L powders in 3D printing process. Powder Technol. 2020;47:1113.
[16] Alonso B, Capella W, Dorador J, Ekdale AA, Grove C, Lauridsen BW. Introducing Fiji and icy image processing techniques in iconological research as a tool for Sedimentary Basin analysis. J Microsc. 2019;413:143.
[17] Lind R. Open-source software for image processing and analysis: Picture this with ImageJ. Microsc Microanal. 2014;20:131.
[18] Jayaprithika A, Mannan M, Santos R, Shafigh P, Yousif E, Adebakin I. Microstructural pore analysis using SEM and ImageJ on the absorption of treated coconut shell aggregate. Constr Build Mater. 2021;324:129217.
[19] Díez M, Jenkins D, Flores B, Grigore M, Patrick J, Lin M. Automated procedure for Coke microstructural characterization in ImageJ software aiming industrial application. Fuel. 2021;304:121374.
[20] Hu Y, Hanning C, Xiaohui J, Xiaodan L, Jianbo L. Heat treatment of titanium manufactured by selective laser melting: Microstructure and tensile properties. J Mat Res Tech. 2022;18:245.
[21] Sharon S, Olukayode O, Eugene O, Apata O. Additive manufacturing of titanium-based alloys - a review of methods, properties, challenges, prospects. Mater Today Commun. 2022;8:e09041.
[22] Alexandra A, Robert F, Thomas E, Florian P. Powder metallurgy strategies to improve properties and processing of Titanium alloy. Powder Metall. 2017;19:1600743.
[23] Wang D, Linqing L, Guowei D. Recent progress on additive manufacturing of multi-material structures with laser powder bed fusion. Prog Addit Manuf. 2022;13:329.
[24] Sanforda L, Jaafara I, Seibia A, Gohnb A. The effect of infill angle, build orientation, and void fraction on the tensile strength and fracture of 3D printed ASA via fused filament fabrication. Mater Lett. 2022;33:569.
[25] Wang J, Guo X, Qin J, Zhang D, Lu W, Fernández A. Microstructure and mechanical properties of investment casted titanium matrix composites with B4C additions. Mat Sci Eng A. 2015;628:366.
[26] Kang N, Coddet P, Liao H, Coddet C. The effect of heat treatment on microstructure and tensile properties of cold spray Zr base metal glass/Cu composite. Surf Coat Tech. 2015;280:64.